Energy transfer from an electron-hole plasma layer to a quantum well in semiconductor structures

S. K. Lyo
Sandia National Laboratories, Albuquerque, New Mexico 87185, USA
(Received 4 December 2009; revised manuscript received 8 February 2010; published 3 March 2010)

We investigate the energy-transfer rate from a quasi-two-dimensional (2D) quantum well with an electron-hole plasma to an empty quantum well separated by a wide barrier through dipole-dipole interaction. The rates are compared and contrasted with the 2D-2D transfer rates of classical excitons studied previously. The temperature dependence of the 2D-2D transfer rate of plasmas is strikingly different from that of excitons in general. The dependences of the rates on the carrier density, the center-to-center distance between the plasma and the quantum well, and the temperature are studied.

DOI: 10.1103/PhysRevB.81.115303 PACS number(s): 71.35.Ee, 78.67.De, 71.35.Cc, 78.20.Bh

I. INTRODUCTION

The energy-transfer dynamics of excitons has been studied for a long time for Frankel excitons.[1–3] Energy transfer of Wannier-Mott excitons between confined systems in semiconductors is becoming increasingly important in modern optoelectronic structures such as light emitting diodes (LEDs) and solid-state-lighting (SSL) devices. In these nanostructures, light energy is stored in the form of excitons and electron-hole (e-h) plasmas which can move between two-dimensional (2D) quantum wells (QWs) as well as in QWs with lower dimensions. While the energy-transfer dynamics of Wannier-Mott excitons between these confined structures are more complicated than that of Frankel excitons due to extra degrees of freedom for the center-of-mass (CM) motion and is not yet fully studied, it is of much practical and academic interest. Exciton transfer between 2D QWs has been studied in the past experimentally[4,5] and theoretically.[4,6,7] Also, exciton transfer between QWs and molecular layers is of current interest.[8,9] Intra-QW transfer of excitons was studied earlier.[10] Excitons can be photogenerated by a laser excitation as well as e-h diffusion. Under an intense laser excitation or an intense e-h current, excitons become an e-h plasma. Since the threshold density and the temperature of the transition from excitons to a plasma is not clear, we investigate, in this paper, what the characteristic differences are in the nature of energy transfer from 2D excitons and from a 2D plasma to an empty QW separated by a thick barrier by studying energy transfer from an e-h plasma and comparing the results from earlier results[6] on exciton transfer. We study the standard Förster[1] coupling mechanism and ignore complex many-body effects.[11–13]

In typical semiconductor structures with wide barriers, energy transfer through tunneling yields a negligible rate. Transfer via thermal activation is also negligible except for systems with shallow barriers at high temperatures.[14] When the two QWs are not too far, the so-called Förster (i.e., dipole-dipole) mechanism of energy transfer plays a dominant role.[1,2,6] In this case, the transfer rate is expected to decay rapidly as $\sim 1/d^4$ with the center-to-center distance d between the QWs. Surprisingly, past observed data[4,5,15] indicate that the 2D-2D energy-transfer rate decays very slowly with d at a long distance. Recently, the author[6] proposed a photon-exchange mechanism, which yields a weak (e.g., a logarithmic) dependence on d and becomes more important than the dipolar mechanism at a long distance.

In this paper, we investigate the energy-transfer rate from a degenerate and nondegenerate e-h plasma in a QW to an empty QW separated by a wide barrier through the Förster mechanism. We assume that the QWs are narrow and deep with only the ground levels populated. The rates obtained are compared and contrasted with the 2D-2D transfer rates of classical excitons studied previously. The temperature dependence of the transfer rate of plasmas is strikingly different from that of excitons in general. The dependences of the rates on the carrier density, the center-to-center distance between the plasma and the quantum well, and the temperature are studied.

The organization of this paper is as follows. In the next section, we present a basic formalism including the wave functions and the dipolar coupling. The energy-transfer rate is studied for nondegenerate and degenerate plasmas in Sec. III. The transfer rate in the nondegenerate regime is compared and contrasted with that of excitons. In Sec. IV, numerical results are presented and discussions are given. A brief summary is given in Sec. V.

II. BASIC FORMALISM

Energy transfer from an e-h plasma to an adjacent QW is achieved through an annihilation of an e-h pair in the initial QW and a subsequent creation of a new e-h pair in the final QW through dipole-dipole interaction. For Stokes transfer, the extra energy is dissipated into the kinetic energy of the e-h pair, while anti-Stokes transfer is achieved through an energy activation in the initial well. The latter effect is included in the thermal averaging of the initial state. Although only the ground states are considered explicitly for the QWs for simplicity, extensions to excited states are trivial. A free e-h pair moving with 2D wave vectors $\mathbf{k}_e, \mathbf{k}_h$, the CM wave vector $\mathbf{K}$, and the relative wave vector $\mathbf{k}$ is represented as[6]

$$|j,\mathbf{K},\mathbf{k}\rangle = \frac{v_0}{L^2}\sum_{\mathbf{r}_e,\mathbf{r}_h} e^{i\mathbf{K}\cdot\mathbf{R}_{cm\|}-i\mathbf{k}\cdot\mathbf{r}_{eh\|}}F_{zj}(z_e-z_j,z_h-z_j)a^{\dagger}_{c\mathbf{r}_e}a_{v\mathbf{r}_h}|0\rangle, \tag{1}$$

where $\mathbf{k}_e=\alpha_e\mathbf{K}-\mathbf{k}$, $\mathbf{k}_h=\alpha_h\mathbf{K}+\mathbf{k}$, and $F_{zj}(z_e-z_j,z_h-z_j)$ is the product of the electron and hole confinement envelop wave

functions. The wave vectors are 2D vectors in the QW plane. In Eq. (1), $\Omega=L^3=Nv_0$ is the sample volume, v_0 is the unit-cell volume, N is the total number of the unit cells, $|0\rangle$ signifies the vacuum state with an empty conduction band (c) and filled valence band (v), and z_j is the z coordinate in the perpendicular (growth) direction at the center of the QW. The electron and hole coordinates are given by $\mathbf{r}_e=(\mathbf{r}_{e\|},z_e)$ and $\mathbf{r}_h=(\mathbf{r}_{h\|},z_h)$, respectively. In the QW plane, $\mathbf{r}_{eh\|}=\mathbf{r}_{e\|}-\mathbf{r}_{h\|}$ is the 2D relative coordinate, while $\mathbf{R}_{cm\|}=\alpha_e\mathbf{r}_{e\|}+\alpha_h\mathbf{r}_{h\|}$ is the center-of-mass (CM) coordinate. Here, $\alpha_e=m_e/M, \alpha_h=m_h/M$, where m_e (m_h) is the effective mass of the electron (hole) in the plane and $M=m_e+m_h$. The creation and destruction operators $a^\dagger_{c\mathbf{r}_e}$ and $a_{c\mathbf{r}_e}$ ($a^\dagger_{v\mathbf{r}_h}$ and $a_{v\mathbf{r}_h}$) creates and destroys an electron in the conduction (valence) band at the position $\mathbf{r}_e$ ($\mathbf{r}_h$) in the Wannier representation. The normalization condition of the wave function is given by $\langle j',\mathbf{K}',\mathbf{k}'|j,\mathbf{K},\mathbf{k}\rangle=\delta_{j,j'}\delta_{\mathbf{K}',\mathbf{K}}\delta_{\mathbf{k}',\mathbf{k}}$ with $\int dz_e\int dz_h|F_{zj}(z_e,z_h)|^2\equiv 1$ in view of $\Sigma_{\mathbf{r}_\sigma}\to\int d^3r_\sigma/v_0$. Here, the overlap between the confinement wave functions of the two QWs is neglected and $\sigma=e,h$, respectively, for the electron and hole representation of the carriers as well as for the conduction and the valence band for the simplicity of the notation. Note that $\varepsilon_e(k_e)+\varepsilon_h(k_h)=E_M(K)+\varepsilon_\mu(k)$, where we define

$$\varepsilon_e(k_e)=\frac{(\hbar k_e)^2}{2m_e},\quad \varepsilon_h(k_h)=\frac{(\hbar k_h)^2}{2m_h},$$

$$\varepsilon_\mu(k)=\frac{(\hbar k)^2}{2m_\mu},\quad E_M(K)=\frac{(\hbar K)^2}{2M}. \tag{2}$$

Here, μ is the reduced mass.

The electron-electron interaction is given by

$$H_{ee}=\frac{1}{2\kappa}\int d^3r\int d^3r'\,\hat{\psi}^\dagger(\mathbf{r})\hat{\psi}^\dagger(\mathbf{r}')\frac{e^2}{|\mathbf{r}-\mathbf{r}'|}\hat{\psi}(\mathbf{r}')\hat{\psi}(\mathbf{r}), \tag{3}$$

where κ is the bulk dielectric constant and $\hat{\psi}(\mathbf{r})$ is a field operator

$$\hat{\psi}(\mathbf{r})=\sum_\sigma \phi_\sigma(\mathbf{r})a_{\sigma\mathbf{r}_\sigma}, \tag{4}$$

where $\phi_\sigma(\mathbf{r})$ is the Wannier function with $\mathbf{r}=0$ at the center of the cell. Using Eqs. (1), (3), and (4), we find after a lengthy algebra

$$\langle 2,\mathbf{K}',\mathbf{k}'|H_{ee}|1,\mathbf{K},\mathbf{k}\rangle=\delta_{\mathbf{K},\mathbf{K}'}\frac{1}{A}\int dz\int dz'\,C(\mathbf{K},R_z)\times F^*_{z2}(z',z')F_{z1}(z,z), \tag{5}$$

where $A=L^2$ is the cross sectional area of the QW and

$$C(\mathbf{K},R_z)=\int d^2R_\|e^{i\mathbf{K}\cdot\mathbf{R}_\|}\frac{e^2}{\kappa R^3}[\mathbf{D}_1\cdot\mathbf{D}_2^*-3(\hat{\mathbf{R}}\cdot\mathbf{D}_1)(\hat{\mathbf{R}}\cdot\mathbf{D}_2^*)]. \tag{6}$$

The effect of the dipole-dipole coupling between excitons in a similar double-QW system on phonon-assisted interwell exciton transfer, luminescence and other properties was studied earlier.[16] The transition dipole moment is given by

$$\mathbf{D}_j=\int_{\text{cell}}\phi^*_{vj}(\mathbf{r})\mathbf{r}\phi_{cj}(\mathbf{r})d^3r. \tag{7}$$

The quantity $\hat{\mathbf{R}}=\mathbf{R}/R$ is a unit vector, where $\mathbf{R}$ is a three-dimensional vector with an in-plane component $\mathbf{R}_\|$ and a magnitude $R=|\mathbf{R}|=\sqrt{R_\|^2+R_z^2}$. Here, $R_z=|z-z'+d|$. The quantity $C(\mathbf{K},R_z)$ is given by[6,16,17]

$$C(\mathbf{K},R_z)=(\pi D_1D_2e^2/\kappa)Ke^{-K|R_z|}\Phi(\phi_\mathbf{K}), \tag{8}$$

where $\Phi(\phi_\mathbf{K})=\cos(2\phi_\mathbf{K}-\phi_D)+\cos\phi_D$ and $\phi_\mathbf{K}(\phi_D)$ is the angle between $\mathbf{K}$ and $\mathbf{D}_1$ ($\mathbf{D}_1$ and $\mathbf{D}_2$) assumed to be in the QW plane. Note that $C(\mathbf{K},R_z)=0$ at $K=0$ reflecting the fact that the Coulomb interaction between a charge and uniformly distributed dipoles vanishes. The matrix element in Eq. (5) is independent of $\mathbf{k}$ and $\mathbf{k}'$. This quantity can be written as

$$\langle 2,\mathbf{K}',\mathbf{k}'|H_{ee}|1,\mathbf{K},\mathbf{k}\rangle=\delta_{\mathbf{K},\mathbf{K}'}\frac{1}{A}C(\mathbf{K},d)S(Kd), \tag{9}$$

where

$$S(Kd)=\exp(Kd)\int dz\int dz'\,\exp(-KR_z)\times F^*_{z2}(z',z')F_{z1}(z,z). \tag{10}$$

The function $S(Kd)$ approaches unity, when the distance d is much greater than the QW widths.[6]

III. ENERGY-TRANSFER RATE

Energy transfer goes through a process where an electron and a hole in the plasma with wave numbers $\mathbf{k}_e,\mathbf{k}_h$ and a total energy $\varepsilon_e(\mathbf{k}_e)+\varepsilon_h(\mathbf{k}_h)=\varepsilon_\mu(\mathbf{k})+E_M(\mathbf{K})$ are annihilated in the initial QW, creating a new pair with wave numbers $\mathbf{k}'_e,\mathbf{k}'_h$ and a total energy $\varepsilon_e(\mathbf{k}'_e)+\varepsilon_h(\mathbf{k}'_h)=\varepsilon_\mu(\mathbf{k}')+E_M(\mathbf{K}')$ in the final empty well. These final electrons and holes relax rapidly (e.g., within a picosecond) to the ground state in a time scale much shorter than the energy-transfer time, eventually forming excitons. The average transfer rate $W_{1\to2}$ per e-h pair is given, in view of $\mathbf{K}'=\mathbf{K}$, by

$$\mathcal{N}W_{1\to2}=\frac{4\pi}{\hbar}\sum_{\mathbf{k}_e,\mathbf{k}_h,\mathbf{k}'}f_e(\mathbf{k}_e)f_h(\mathbf{k}_h)|V(K,d)|^2\times\delta(\varepsilon_\mu(\mathbf{k})-\varepsilon_\mu(\mathbf{k}')+p\Delta), \tag{11}$$

where $f_\sigma(\mathbf{k}_\sigma)$ is the Fermi function. The chemical potentials μ_σ are given by $\mu_\sigma=k_BT\ln[e^{T_{\sigma F}/T}-1]$ for a single level occupation, where $T_{\sigma F}=\pi\hbar^2N_{2D}/m_\sigma$ is the Fermi temperature, $N_{2D}=\mathcal{N}/A$ is the 2D electron and hole density, and $\mathcal{N}$ is the number of the e-h pairs.[18] In Eq. (11), Δ is the energy mismatch between the two ground-state confinement levels, $V(K,d)=\langle 2,\mathbf{K}',\mathbf{k}'|H_{ee}|1,\mathbf{K},\mathbf{k}\rangle$ is independent of $\mathbf{k}$ and $\mathbf{k}'$. The quantity p equals $p=1(-1)$, if the ground level of QW1 is higher (lower) than that of QW2. The prefactor of the rate includes the sum over the spin degeneracy. The rate given in Eq. (11) includes only the direct e-h exchange processes between the two QWs and ignores higher-order perturbative

inelastic (e.g., phonon-assisted) processes, which are expected to yield subsidiary contributions.

The summation on $\mathbf{k}'$ in Eq. (11) yields

$$W_{1\to 2}=\frac{4\pi}{\hbar\mathcal{N}}\frac{Am_\mu}{2\pi\hbar^2}\sum_{\mathbf{k},\mathbf{K}}u(\varepsilon_\mu(\mathbf{k})+p\Delta)f_e(\mathbf{k}_e)f_h(\mathbf{k}_h)|V(K,d)|^2, \tag{12}$$

where $u(x)$ is a unit step function. We note here that dielectric screening for the transition dipole moment $\mathbf{D}_1$ in the plasma is neglected due to the fact that $\mathbf{D}_1$ admixes a small perturbation of the order $D_1\phi_v(\mathbf{r})(D_1\phi_c(\mathbf{r}))$ to the conduction (valence) wave function $\phi_c(\mathbf{r})(\phi_v(\mathbf{r}))$ and causes no charge-density perturbation to the first order in D_1 in the conduction (valence) band due to the orthogonality of $\phi_c(\mathbf{r})$ and $\phi_v(\mathbf{r})$.

A. Nondegenerate plasmas

While a nondegenerate model is applicable only at low e-h densities and high temperatures (i.e., $T\gg T_{\sigma F}$), it is still interesting to look into its predictions not only for the simplicity of the results but also because it is useful to compare the rate with the well-known behavior of excitons. The result shows that the temperature dependence of the transfer rate of a nondegenerate plasma is the same as that of excitons except for a proportionality constant. We use

$$f_e(\mathbf{k}_e)f_h(\mathbf{k}_h)=\frac{1}{Z}\exp\{-\beta[\varepsilon_e(\mathbf{k}_e)+\varepsilon_h(\mathbf{k}_h)]\}$$
$$=\frac{1}{Z}\exp\{-\beta[\varepsilon_\mu(\mathbf{k})+E_M(K)]\}, \tag{13}$$

where $Z=Z_eZ_h$ with

$$Z_\sigma=\frac{m_\sigma k_BT}{\pi\hbar^2N_{2D}}. \tag{14}$$

The sums over $\mathbf{k}_e,\mathbf{k}_h$ in Eq. (13) can be replaced by those over the new independent variables $\mathbf{k},\mathbf{K}$, yielding

$$W_{1\to 2}=\frac{4\pi}{\hbar\mathcal{N}}\frac{Am_\mu}{2\pi\hbar^2}\frac{1}{Z}\sum_{\mathbf{k},\mathbf{K}}u(\varepsilon_\mu(\mathbf{k})+p\Delta)e^{-\beta(\varepsilon_\mu(\mathbf{k})+E_M(K))}$$
$$\times|V(K,d)|^2. \tag{15}$$

Defining $\Delta_-=0$ ($\Delta_-=\Delta$) for $p=1$ ($p=-1$), we find

$$W_{1\to 2}=\frac{N_{2D}m_\mu A^2}{2\hbar Mk_BT}\exp(-\beta\Delta_-)\int_0^\infty KdK\exp[-\beta E_M(K)]$$
$$\times|V(K,d)|^2. \tag{16}$$

The rate increases linearly with N_{2D} in this nondegenerate regime. In the degenerate regime, however, the rate increases sublinearly and saturates at high densities as will be shown later.

Dipole interaction yields[6] $\langle\Phi(\phi_{\mathbf{K}})^2\rangle=2$ and

$$|V_{dip}(K,d)|^2=\frac{2}{A^2}(\pi D_1D_2e^2/\kappa)^2K^2e^{-2K|R_z|}S(Kd)^2, \tag{17}$$

resulting in

$$W_{1\to 2}=\frac{N_{2D}m_\mu}{\hbar Mk_BT}\left(\frac{\pi D_1D_2e^2}{\kappa}\right)^2\exp(-\beta\Delta_-)$$
$$\times\int_0^\infty K^3dKe^{-\beta E_M(K)-2Kd}S(Kd)^2. \tag{18}$$

For a large d, the cutoff for the K-integration arises from $1/d$. A dimensional analysis indicates that $W_{1\to 2}\propto 1/d^4$ for a large distance d. Defining $\xi_T=\hbar/\sqrt{2Mk_BT}$, we find

$$W_{1\to 2}=W_{eh}\exp(-\beta\Delta_-)\int_0^\infty x^3dxe^{-x^2-2xd/\xi_T}S(xd/\xi_T)^2, \tag{19}$$

where

$$W_{eh}=\frac{2\pi^2N_{2D}m_\mu}{\hbar^3}\left(\frac{D_1D_2e^2}{\kappa\xi_T}\right)^2. \tag{20}$$

A very similar result was obtained earlier[6] for the thermally averaged dipolar transfer rate $W^{ex}_{1\to 2}$ of a single exciton from QW1 to QW2,

$$W^{ex}_{1\to 2}=W_{ex}\exp(-\beta\Delta_-)\int_0^\infty x^3dxe^{-x^2-2xd/\xi_T}S(xd/\xi_T)^2, \tag{21}$$

where the coefficient W_{eh} in Eq. (19) is replaced with

$$W_{ex}=\frac{32\pi m_\mu}{\hbar^3}\left(\frac{D_1D_2e^2}{\kappa a_B\xi_T}\right)^2. \tag{22}$$

Here, a_B is the Bohr radius of the exciton in the bulk. The ratio of these two rates equals

$$R^{eh}_{ex}\equiv\frac{W_{eh}}{W_{ex}}=\frac{\pi N_{2D}(a_B/2)^2}{4}. \tag{23}$$

This ratio indicates that the plasmas play a major role for energy transfer when the number of e-h pairs inside the 2D exciton radius $a_B/2$ is much larger than unity. Naturally, excitons will be dissociated into a plasma in this limit.

B. Degenerate plasmas

For a degenerate plasma, we use the expression in Eq. (12). Defining $Y^2=E_M(K),y^2=\varepsilon_\mu(k)$, we write

$$\varepsilon_e(\mathbf{k}_e)=(\sqrt{\alpha_e}Y-\sqrt{\alpha_h}y)^2+4\sqrt{\alpha_e\alpha_h}yY\sin^2(\psi/2)\equiv\mathcal{E}_e(Y,y,\psi) \tag{24}$$

and

$$\varepsilon_h(\mathbf{k}_h)=(\sqrt{\alpha_h}Y-\sqrt{\alpha_e}y)^2+4\sqrt{\alpha_e\alpha_h}yY\cos^2(\psi/2)$$
$$\equiv\mathcal{E}_h(Y,y,\psi), \tag{25}$$

where ψ is the angle between $\mathbf{K}$ and $\mathbf{k}$ and find

$$W_{1\to 2} = \frac{A^2}{\hbar N_{2D}} \frac{2m_\mu^2 M}{\pi^3 \hbar^6} \int_0^\infty Y dY \int_0^\infty y dy \int_0^\pi d\psi |V(K,d)|^2 \times \frac{u(y^2 + p\Delta)}{\exp[\beta(\mathcal{E}_e(Y,y,\psi) - \mu_e)] + 1} \times \frac{1}{\exp[\beta(\mathcal{E}_h(Y,y,\psi) - \mu_h)] + 1}. \quad (26)$$

For dipolar interaction, we find

$$W_{1\to 2} = \frac{8\pi m_e m_h N_{2D}}{\hbar^5 \varepsilon_{eF} \varepsilon_{hF}} \left(\frac{D_1 D_2 e^2}{\kappa} \right)^2 \int_0^\infty Y^3 dY \times \int_0^\infty y dy \int_0^\pi d\psi u(y^2 + p\Delta) e^{-2Kd} S(Kd)^2 \times \frac{1}{\exp[\beta(\mathcal{E}_e(Y,y,\psi) - \mu_e)] + 1} \times \frac{1}{\exp[\beta(\mathcal{E}_h(Y,y,\psi) - \mu_h)] + 1}. \quad (27)$$

In the high-temperature nondegenerate limit, this result reduces to Eq. (19).

IV. NUMERICAL EVALUATION AND DISCUSSIONS

For a numerical evaluation of the energy-transfer rate, we use the following parameters relevant for GaAS/$Al_{0.3}Ga_{0.7}As$ QWs: $m_e = 0.067 m_0, m_h = 0.14, D_1 = D_2 = 5$ Å, and $\kappa = 12.4$.[6] We study Stokes transfer (i.e., $p=1$) with $\Delta = 60$ meV.[4]

Figure 1 displays the average energy-transfer rate $W_{1\to 2}$ from a plasma in the nondegenerate regime as a function of the temperature at a distance $d = 100$ Å for the 2D electron density $N_{2D} = 5 \times 10^{10}/\text{cm}^2$ (dashed curve). The upper solid curve displays the transfer rate of excitons. The vanishing rates at $T = 0$ K arise from the nondegenerate model where the kinetic energy of the center-of-mass motion vanishes according to the Boltzmann statistics and, at the same time, the dipolar coupling strength vanishes according to Eq. (8) for $K = 0$. However, the results for the e-h plasma in Fig. 1 are not valid at low temperatures, where the plasma becomes degenerate and the rates should saturate toward $T = 0$ K as will be shown in Fig. 2. In contrast, the rates for the excitons vanish at $T = 0$ K due to the vanishing dipolar coupling strength mentioned above after going through a maximum as a function of the decreasing temperature. This is the characteristic behavior of exciton transfer for delocalized excitons. However, the rate does not vanish at $T = 0$ K when the excitons are localized in a disordered QW.[6] The inset in Fig. 1 shows the temperature-independent ratio of the transfer rates of plasmas and excitons, which is linear in N_{2D}. The temperature-dependent rates for other e-h densities can be deduced from their linearity in N_{2D} in the nondegenerate regime. However, these rates are not linear in N_{2D} outside this nondegenerate regime as will be discussed later.

The average energy-transfer rate $W_{1\to 2}$ from a plasma in the degenerate regime is displayed in Fig. 2 as a function of the temperature on the left axis at a distance $d = 100$ Å for the 2D electron densities $N_{2D} = 10^{11}/\text{cm}^2$ (dashed-double-dotted curve), $N_{2D} = 5 \times 10^{11}/\text{cm}^2$ (dashed-dotted curve), $N_{2D} = 10^{12}/\text{cm}^2$ (dashed curve), and $N_{2D} = 2 \times 10^{12}/\text{cm}^2$

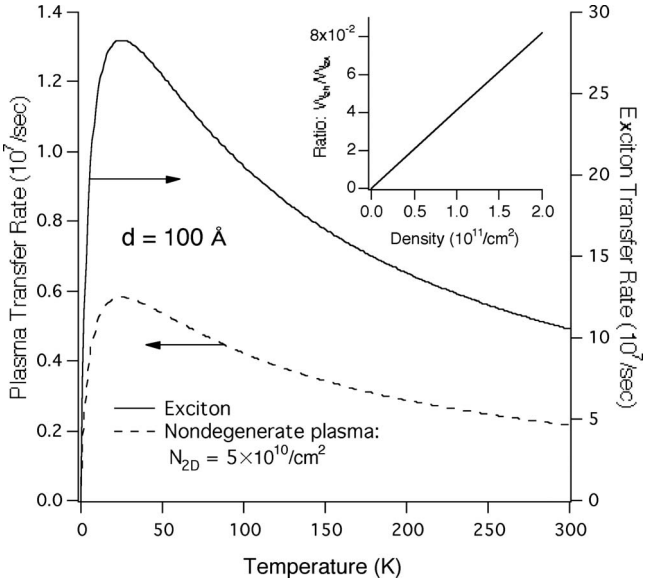

FIG. 1. The average energy-transfer rate $W_{1\to 2}$ from a plasma in a nondegenerate model as a function of the temperature at a distance $d = 100$ Å for the 2D electron densities $N_{2D} = 5 \times 10^{10}/\text{cm}^2$ (dashed curve). In this model, $W_{1\to 2}$ is linear in N_{2D}. The upper solid curve displays the density-independent transfer rate of an exciton at low densities below the plasma-exciton transition. The inset shows the ratio in Eq. (23) of the transfer rates of excitons and a nondegenerate plasma as a function of N_{2D}.

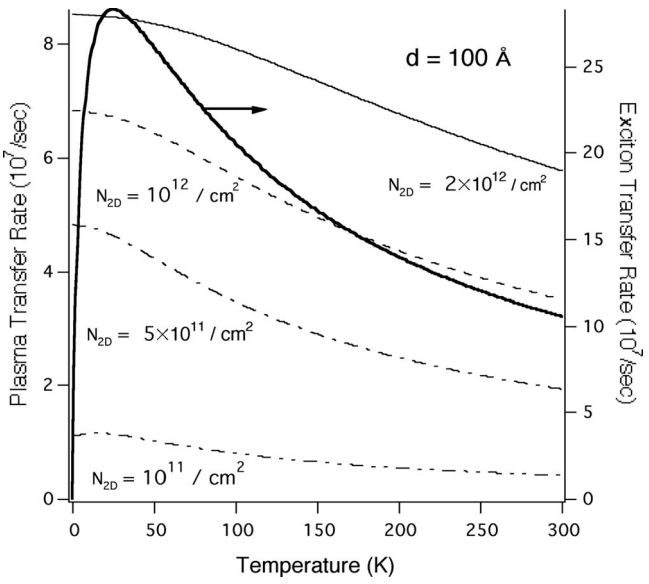

FIG. 2. The average energy-transfer rate $W_{1\to 2}$ from a plasma in the degenerate regime (left axis) as a function of the temperature at a distance $d = 100$ Å for the 2D electron densities $N_{2D} = 10^{11}/\text{cm}^2$ (dashed-double-dotted curve), $N_{2D} = 5 \times 10^{11}/\text{cm}^2$ (dashed-dotted curve), $N_{2D} = 10^{12}/\text{cm}^2$ (dashed curve), and $N_{2D} = 2 \times 10^{12}/\text{cm}^2$ (solid curve). The thick solid curve indicates the exciton transfer rate (right axis), which was also shown in Fig. 1.

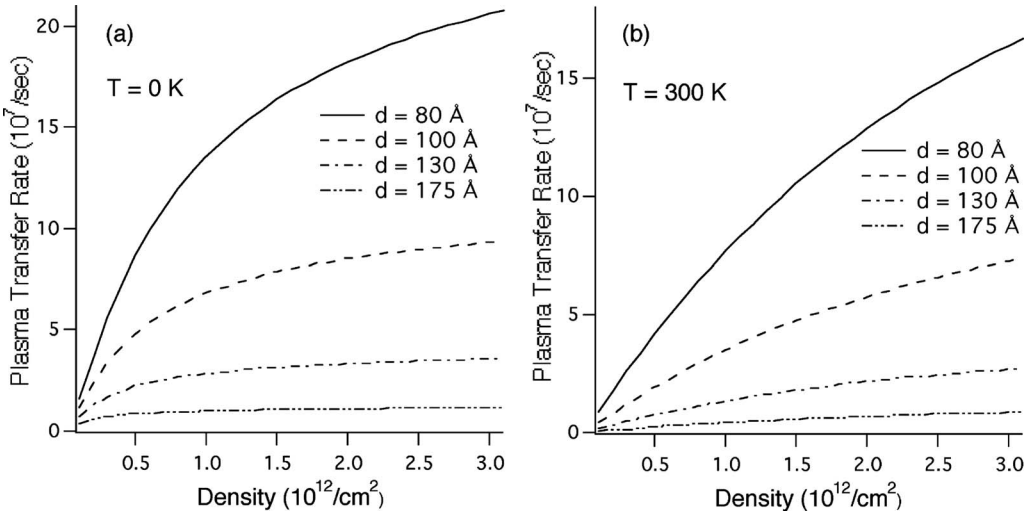

FIG. 3. The average energy-transfer rate $W_{1\to 2}$ from a plasma in the degenerate regime as a function of the 2D electron density N_{2D} at (a) $T=0$ K and (b) $T=300$ K for the distances $d=80$ Å (solid curve), $d=100$ Å (dashed curve), $d=130$ Å (dashed-dotted curve), and $d=175$ Å (dashed-double-dotted curve).

(solid curve). The density-independent exciton transfer rate is also shown on the right axis (thick solid curve) for comparison and is the same as that displayed in Fig. 1. While the average transfer rate $W_{1\to 2}$ from the plasma is smaller than the rate of an exction, it increases as a function of the density and will be important at high densities. Furthermore, the excitons will dissociate into an e-h plasma at high densities. The question of the exciton-plasma transition density and the temperature is beyond the scope of this study and will not be discussed here. Note that the transfer rates for the plasmas saturate at low temperatures in striking contrast to the vanishing rates of the excitons at $T=0$ K. The plasma transfer rates in Fig. 2 become nearly "parallel" to the exciton transfer rate at high temperatures, where they become nearly linear in N_{2D} at $N_{2D}=10^{11}/\mathrm{cm}^2$, indicating that nondegenerate behavior begins to appear only for the low densities near or beyond the high end of the temperature range of Fig. 2.

Naively speaking, one may think that the plasma transfer rate, originating from a two-particle process, may be linear in the density. However, this is not true in general because the transfer-matrix element depends linearly on the center-of-mass wave vector K for small K with the maximum K restricted by the maximum kinetic energy of the occupied states determined by $K^2\sim(2k_F)^2\sim N_{2D}$. One might then expect that the transfer rate will increase rapidly with the density N_{2D} because large electron and hole wave numbers just inside the Fermi surface will contribute to strong-coupling strengths through the large values of K. However, this effect is impeded at high densities due to the momentum cutoff factor $K\simeq 1/d$ discussed earlier. Therefore, electrons and holes in a high-density plasma with large wave numbers beyond this cutoff value do not contribute to the transfer processes, resulting in the saturation of the rate. This effect is demonstrated in Fig. 3(a), where the average energy-transfer rate from a plasma at $T=0$ K is displayed as a function of N_{2D} for the distances $d=80$ Å (solid curve), $d=100$ Å (dashed curve), $d=130$ Å (dashed-dotted curve), and $d=175$ Å (dashed-double-dotted curve). Clearly, the rate begins to show early tendency toward saturation at a smaller density at a larger distance when the Fermi wave numbers reach $k_{\sigma F}=\sqrt{2\pi N_{2D}}\sim 1/d$. It should be noted here that the result in Fig. 3(a) is not valid at very low densities, where the electrons and holes will bind into excitons, yielding much larger transfer rate as shown in Fig. 1. The saturation behavior is less pronounced at high temperatures where maximum K is determined by T rather than N_{2D} due to the thermal smearing of the Fermi surface as shown in Fig. 3(a) at $T=300$ K in Fig. 3(b). Also, the rate decreases monotonically with the increasing temperature, owing to the fact that more carriers have wave vectors K that cross over the cutoff value $\sim 1/d$.

The total 2D-2D energy-transfer power of the plasma per area is given by $\mathcal{P}_{1\to 2}=W_{1\to 2}(E_g-\Delta)N_{2D}$, where E_g is the energy gap. This quantity is plotted in Fig. 4(a) at $T=0$ K and Fig. 4(b) at $T=300$ K as a function of the 2D density N_{2D} for several distances $d=80$, 100, 130, and 175 Å. The magnitude of the power is significant enough to be relevant for SSL applications. It decreases gradually as a function of the rising temperature due to the temperature dependence of $W_{1\to 2}$ discussed in the preceding paragraph for Fig. 3.

Figure 5 displays a log-log plot of the average energy-transfer rate from a plasma in the degenerate regime as a function of the distance d for the 2D electron densities $N_{2D}=10^{11}/\mathrm{cm}^2$ (black solid circles), $N_{2D}=5\times 10^{11}/\mathrm{cm}^2$ (blue solid squares), and $N_{2D}=10^{12}/\mathrm{cm}^2$ (red solid triangles) for the temperatures $T=0$ K (solid curves), $T=100$ K (dashed curves), and $T=300$ K (dashed-dotted curves). The dotted curve at the bottom with a green open inverted triangle indicates the $1/d^4$ dependence. The deviation from the $1/d^4$ dependence is clearly visible at short distances at low densities and low temperatures, for example, at $N_{2D}=10^{11}/\mathrm{cm}^2$ at 0 K (represented by the black solid curve with a black solid circle) due to the small kinetic energies of the carriers with $K<1/d$. The asymptotic behavior $\propto 1/d^4$ is reached at large d and at high densities when the wave numbers of the high-energy carriers exceed the $K>1/d$ limit.

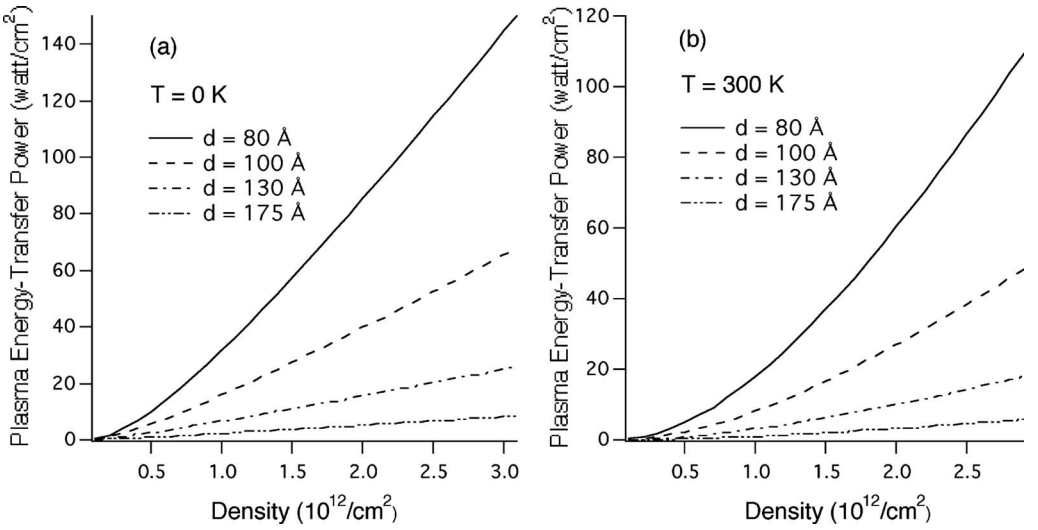

FIG. 4. The power $\mathcal{P}_{1\to 2}$ of energy transfer per area from a plasma at (a) $T=0$ K and (b) $T=300$ K as a function of the 2D density N_{2D} at several distances $d=80$ Å (solid curve), $d=100$ Å (dashed curve), $d=130$ Å (dashed-dotted curve), and $d=175$ Å (dashed-double-dotted curve).

This asymptotic limit is more readily reached at higher densities or/and higher temperatures as seen from the figure.

V. CONCLUSIONS

We have investigated the energy-transfer rate from a quasi-two-dimensional plasma to an empty quantum well through the standard dipolar coupling. The rates were compared and contrasted with the 2D-2D transfer rates of classic excitons studied previously. The dependence of the rate on the carrier density, the distance between the quantum wells and the temperature was studied. The power of the total 2D-2D energy transfer was also calculated and is shown to be significantly large to be relevant for applications for solid-state-lighting devices.

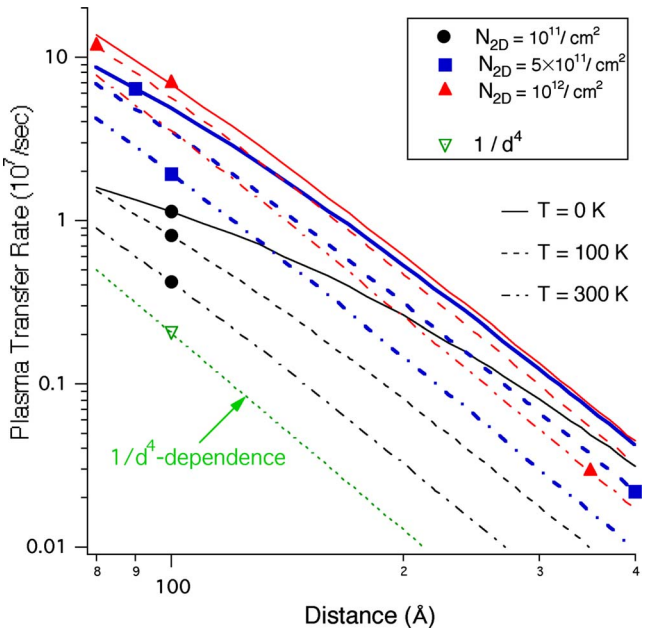

FIG. 5. (Color online) A log-log plot of the average energy-transfer rate $W_{1\to 2}$ from a plasma in the degenerate regime as a function of the distance d for the 2D electron densities $N_{2D}=10^{11}/\mathrm{cm}^2$ (black solid circles), $N_{2D}=5\times 10^{11}/\mathrm{cm}^2$ (blue solid squares), and $N_{2D}=10^{12}/\mathrm{cm}^2$ (red solid triangles) for the temperatures $T=0$ K (solid curves), $T=100$ K (dashed curves), and $T=300$ K (dashed-dotted curves). The dashed-double-dotted curve at the bottom with a green open triangle indicates a $1/d^4$ dependence.

At a low temperature, electrons and holes bind into excitons and yield a large energy-transfer rate due to the proximity of the electron and the hole inside an exciton. The rate is independent of the exciton density. As the density increases, excitons dissociate into a plasma even at low temperatures. The average transfer rate of the plasma increases with the density, reflecting the two-particle nature of the transfer. However, the increase is not simply linear in the density as one might expect intuitively. It increases sublinearly with the density and saturates at high densities. This arises from the fact that the interwell coupling strength depends on the total momentum K as well as the well-to-well distance d which affect the density dependence. These effects are demonstrated in the density dependence of the rates in Fig. 3. We also found a significant 2D-2D energy-transfer power from a plasma as displayed in Fig. 4.

The transfer rate increases with the carrier density and begins to saturate at a density where the Fermi wave numbers reach the cutoff wave number $\sim 1/d$ at zero temperature. In these regimes, the rate shows the asymptotic dependence $\propto 1/d^4$ shown in Fig. 5. This limiting behavior is

The temperature dependence of the 2D-2D transfer rate of a plasma was found to be very different from that of an exciton at low temperatures due to the different statistics of plasmas and excitons, while it is similar in the high-temperature nondegenerate regime. As the temperature is lowered toward $T=0$ K, the 2D-2D transfer rate of a plasma rises steadily and saturates at a nonzero value, while the exciton transfer rate reaches a peak and then decreases, vanishing at $T=0$ K as shown in Fig. 2.

reached at a closer distance at higher temperatures, where there are many e-h pairs with large center-of-mass wave numbers K exceeding the cutoff value $1/d$.

In this paper, we have studied interwell energy transfer of plasmas as a first step toward understanding most efficient energy-transfer processes in confined structures, which have promising applications to SSL devices. Here, optical energy is supplied through the diffusion current of the electrons and holes into QWs, creating excitons or plasmas. The next step is to transfer this energy to efficient light emitters. Nanoscale quantum dots localize and confine electrons and holes in a close proximity and yield large oscillator strengths. Therefore, energy transfer from QWs to dots is expected to be important[8] and is currently under study. The dependences of the rates on the temperature, the density, and the distance d obtained in this paper are unique to the dipolar nature of the coupling. They will be different for the so-called photon-exchange coupling which is much weaker but has a long range. This interaction can be relatively more important at a long distance and will be the subject of a future study.[6]

ACKNOWLEDGMENTS

This work was supported by the U.S. Department of Energy, Office of Science, Office of Basic Energy Sciences through the Energy Frontier Research Center (EFRC) for Solid-State Lighting Science and the Electronic Materials program. Sandia National Laboratories is a multiprogram laboratory operated by Sandia Corporation, a Lockheed-Martin Co., for the U.S. Department of Energy under Contract No. DE-AC04-94AL85000.

[1] Th. Förster, Ann. Phys. (Leipzig) **2**, 55 (1948).
[2] D. L. Dexter, J. Chem. Phys. **21**, 836 (1953).
[3] For a review, see *Laser Spectroscopy in Solids*, 2nd ed., Topics in Applied Physics, edited by W. M. Yen and P. Selzer (Springer-Verlag, New York, 1986), Vol. 49.
[4] A. Tomita, J. Shah, and R. S. Knox, Phys. Rev. B **53**, 10793 (1996).
[5] D. S. Kim, H. S. Ko, Y. M. Kim, S. J. Rhee, S. C. Hohng, Y. H. Yee, W. S. Kim, J. C. Woo, H. J. Choi, J. Ihm, D. H. Woo, and K. N. Kang, Phys. Rev. B **54**, 14580 (1996).
[6] S. K. Lyo, Phys. Rev. B **62**, 13641 (2000).
[7] S. K. Lyo, Phys. Rev. B **64**, 201317(R) (2001).
[8] M. Achermann, M. A. Petruska, S. Kos, D. L. Smith, D. D. Koleske, and V. I. Klimov, Nature (London) **429**, 642 (2004).
[9] D. Basko, G. C. La Rocca, F. Bassani, and V. M. Agranovich, Eur. Phys. J. B **8**, 353 (1999).
[10] T. Takagahara, Phys. Rev. B **31**, 6552 (1985).
[11] R. A. Kaindl, M. A. Camahan, D. Haegelle, R. Loevenich, and D. S. Chemla, Nature (London) **423**, 734 (2003).
[12] J. Szczytko, L. Kappei, J. Berney, F. Morier-Genoud, M. T. Portella-Oberli, and B. Deveaud, Phys. Rev. Lett. **93**, 137401 (2004).
[13] S. Chatterjee, C. Ell, S. Mosor, G. Khitrova, H. M. Gibbs, W. Hoyer, M. Kira, S. W. Koch, J. P. Prineas, and H. Stolz, Phys. Rev. Lett. **92**, 067402 (2004).
[14] H. X. Jiang, E. X. Ping, P. Zhou, and J. Y. Lin, Phys. Rev. B **41**, 12949 (1990).
[15] K. F. Karlsson, H. Weman, K. Leifer, A. Rudra, E. Kapon, and S. K. Lyo, Appl. Phys. Lett. **90**, 101108 (2007).
[16] M. Batsch, T. Meier, P. Thomas, M. Lindberg, S. W. Koch, and J. Shah, Phys. Rev. B **48**, 11817 (1993).
[17] B. S. Wang and J. L. Birman, Phys. Rev. B **43**, 12458 (1991).
[18] While the numbers of electrons and holes are assumed to be equal here, the current formalism can be readily extended to a general case where they are unequal.